

1 **Hydrological processes and permafrost regulate magnitude, source**
2 **and chemical characteristics of dissolved organic carbon export in a**
3 **peatland catchment of northeastern China**

4

5 Yuedong Guo¹, Changchun Song^{1,*}, Wenwen Tan¹, Xianwei Wang¹, Yongzheng Lu¹

6 ¹Key Laboratory of Wetland Ecology and Environment, Northeast Institute of
7 Geography and Agroecology, Chinese Academy of Sciences, Changchun 130012,
8 China

9 Tel: 86-431-85542211

10 Fax: 86-431-85542298

11 Address:

12 Northeast institute of Geography and Agroecology, Chinese Academy of Sciences.
13 No.4888, Shengbei Road, Changchun, Jilin Province, China, 086-130102

14

15 **Abstract**

16 Permafrost thawing in peatlands has the potential to alter the catchment
17 export of dissolved organic carbon (DOC), thus influencing the carbon
18 balance and cycling in linked aquatic and ocean ecosystems. Peatlands
19 along the southern margins of the Eurasian permafrost are relatively

20 understudied despite the considerable risks associated with permafrost
21 degradation due to climate warming. This study examined dynamics of
22 DOC export from a permafrost peatland catchment located in northeastern
23 China during the 2012 to 2014 growing seasons. The estimated annual
24 DOC loads varied greatly between 3211 to 19022 Kg yr⁻¹ with a mean
25 DOC yield of 4.7 g m⁻² yr⁻¹. Although the estimated DOC yield was in the
26 lower range compared with other permafrost regions, it was still significant
27 for the net carbon balance in the studied catchment. There were strong
28 linkages between daily discharge and DOC concentrations in both wet and
29 dry years, suggesting a transport-limited process of DOC delivery from the
30 catchment. Discharge explained the majority of both seasonal and inter-
31 annual variations of DOC concentrations, which made annual discharge a
32 good indicator of total DOC load from the catchment. As indicated by three
33 fluorescence indices, DOC source and chemical characteristics tracked the
34 shift of flowpaths during runoff processes closely. Interactions between the
35 flowpath and DOC chemical characteristics were greatly influenced by the
36 seasonal thawing of the soil active layer. The deepening of the active layer
37 due to climate warming likely increases the proportion of microbial-
38 originated DOC in baseflow discharge.

39

40 **1. Introduction**

41 Permafrost soils have acted as sinks for atmospheric carbon (C) since
42 at least the late Pleistocene and serve as key sources of dissolved organic
43 carbon (DOC) for linked aquatic and ocean ecosystems (Opsahl et al., 1999;
44 Kicklighter et al., 2013). Because changes in the quantity and quality of
45 exported DOC can greatly alter the energy cycles of the linked oceans,
46 considerable progress has been made in recent years to better evaluate
47 potential changes in DOC export patterns from permafrost regions
48 (Townsend-Small et al., 2011; Vonk et al., 2013). However, uncertainties
49 remain regarding the primary drivers and the fate of DOC due to complex
50 interactions between hydrological and thermal dynamics as well as bio-
51 chemical drivers (Olefeldt and Roulet, 2012; Kicklighter et al., 2013).

52 Significant losses of near-surface permafrost have been observed over
53 the past century and such outcomes have induced considerable changes in
54 hydrological processes and soil thermal regimes (Lyon et al., 2009; Lessels
55 et al., 2015), in turn altering the magnitude and timing of terrestrial DOC
56 export processes. Flow pathway is an important and well-documented
57 regulator of DOC export from permafrost regions (Ågren et al., 2010; Guo
58 et al., 2015). Owing to increased levels of hydrological access to previously
59 frozen soils following permafrost degradation, DOC export was forecast to
60 increase in Siberian rivers along a latitudinal transect (Frey and
61 MacClelland, 2009). However, permafrost degradation also increased the
62 likelihood of interactions between subsurface flows and mineral soils,

63 which should lead to considerable DOC absorption by fine soil particles
64 and in turn decrease in DOC export magnitude (Petronne et al., 2006; Striegl
65 et al., 2005). There were significant disparities in DOC export
66 concentrations and seasonal patterns between surface- and subsurface-
67 dominated runoff processes in permafrost catchments (Laudon et al., 2011).
68 The capacity for DOC export from permafrost soils was closely linked to
69 lateral subsurface flow (Striegl et al., 2007; Lyon et al., 2010). Therefore,
70 alterations to flow pathways during permafrost freeze-thaw cycles are
71 some of the most important factors to consider in evaluating DOC export
72 potential in a peatland.

73 Flow pathways also determine chemical composition of the DOC
74 exported from permafrost catchments, which in turn can influence
75 downstream DOC mineralization rates and carbon emissions from streams,
76 lakes and oceans (Mann et al., 2012; Cory et al., 2014). DOC composition
77 can be by flow pathways along the organic-mineral soil layer. Mineral soil
78 particles preferentially absorbed dissolved organic matter high in aromatic
79 components with large molecular weights or acidic functional groups, and
80 aromatic structures (Kalbitz et al., 2005). In contrast, hydrophilic fatty
81 microbial products with low molecular weights were desorbed and released
82 (Striegl et al., 2005). To date, a partial theoretical framework and methods
83 have been developed to understand alterations in DOC chemical
84 characteristics following permafrost degradation (Spencer et al., 2015).

85 But uncertainties still exist in understanding the entire way hydrological
86 processes affect the magnitude and chemical characteristics of DOC
87 exported from permafrost peatland catchments.

88 Given the high spatial heterogeneity of peatlands and the complexity
89 of hydrological processes in permafrost regions, it is important to
90 understand the magnitude and controls on DOC export in different
91 permafrost regions, especially in the south part of the Eurasian continent
92 where limited research has been performed to date. Our study focused on
93 dynamics of DOC release from the Fukuqi River, a tributary of the Amur
94 River positioned along the northern slopes of the Great Xing'an Mountains
95 in northeastern China. The Great Xing'an Mountains form an important
96 barrier from Siberian cold air masses and monsoons of East Asia. The mean
97 annual temperature of the area has on average increased by 0.3 °C every
98 10 years over the last 50 years, and the thickness of the active layer has
99 increased by 20-40 cm on the southern slopes of the Great Xing'an
100 Mountains from the 1970s to 2000 (Jin et al., 2000). However, few studies
101 have focused on possible consequences of permafrost degradation in this
102 region to date. This work thus investigated potential changes in DOC
103 export patterns by answering the following questions:

104 (1) What is the DOC load transported by discharge from the entire
105 catchment?

106 (2) What is the relationship between runoff processes and concentrations,
107 sources, and chemical characteristics of DOC?

108

109 **2. Approach and methodology**

110 **2.1. Study area**

111 Northern sections of the Great Xing'an Mountains in China are
112 located along the southern margins of the continuous permafrost zone in
113 Eurasia. The area represents the most remote region of the East Asia
114 monsoon of the East Eurasian continent. The region includes
115 approximately 8.245×10^3 km² of natural wetlands, representing a major
116 proportion of cold temperate wetlands and an important reservoir of soil
117 carbon and usable water resources for northeastern China.

118 The Fukuqi River, a second order branch of the Amur River, is located
119 in the continuous permafrost of the northern slope of the Great Xing'an
120 Mountains (Fig. 1). The catchment extends across an area of 287 km² with
121 an annual mean temperature of -4.2 °C and a mean annual precipitation of
122 425 mm (1959-2013). Peatland covers the flat river valley and ranges in
123 altitude from 500 to 580 m. Mountains surround the peatland and have a
124 much steeper slope than the peatland (Fig. 1). The peat layer, which is
125 approximately 0.3-0.4 m thick, is composed of typical organic soil with
126 organic matter levels ranging from 40% to 60% and with porosity levels

127 ranging from 60% to 20% near the surface. According to previous field
128 surveys, the peatlands accounts for more than 90% of the total carbon stock
129 in the catchment but covers only about one-third of the total area. The
130 maximum thaw depth of the active layer, ranging from 60 to 80 cm, occurs
131 usually in early August. Below the peat soil layer is mineral soil with a
132 much lower organic content (< 5%) and soil porosity (< 10%) than the
133 upperpeat soil. Sphagnum mosses (*S.capillifolium*, *S. magellanicum*) and
134 sedges (*Eriophorum vaginatum*) are the dominant vegetation. The growing
135 season is from May until late September. The upland mountains on both
136 sides of the valley are extensively covered by mineral soil and gravels with
137 little organic content due to the continuous logging and frequent fires
138 during the past 60 years. The original coniferous forest has been replaced
139 by planted young *Pinus sylvestris var. mongolica*. The maximum thaw
140 depth of the forest ranges from 80 to 100 cm, which is slightly deeper than
141 the peatland.

142

143 **Fig. 1** Geographic location of the study area.

144

145 **2.2. Sampling and monitoring program**

146 Monitoring was conducted from early May to late September in 2012,
147 2013 and 2014. A gauging station to profile DOC concentrations and

148 hydrological parameters was set for the lower reaches of the Fukuqi River
149 (Fig. 1). Water samples were collected from the stream profile every 1–5
150 days with 200 ml polyethylene bottles. A higher sampling frequency was
151 applied during flood events whereas a lower sampling frequency was using
152 during periods of low water. Soil pore water in the peatland was collected
153 from three sites located 50-100 m away from the main river channel on the
154 8th June, 30th June, 27th July and 25th August in 2013 (Fig. 1). When
155 sampling, 100 ml samples of soil pore water were collected at 10 cm
156 intervals along the active layer using ceramic soil pore water samplers
157 (SIC20, Germany). Porewater was collected from the same 3-5 locations
158 at each of the three sites for each sampling period. Due to the gradual
159 thawing of the active layer during the growing seasons, the maximum
160 sampling depths differed for each of the four sampling periods. The water
161 samples were filtered through a 0.45- μm glass fibre membrane, and stored
162 in 4°C in the dark for at most seven days before analysis using a DOC
163 analyser (C-VCPH, Shimadzu, Japan) (Guo et al., 2014). The river began
164 to freeze after September in each year, and flow under the ice was not
165 detected during the winter.

166 Discharge (Q) from through the gauging profile was calculated by
167 measuring water level and flow velocity automatically using a water level
168 monitor (Odyssey, New Zealand, accuracy: ± 2 mm) and a flow meter
169 (Argonaut-ADV, USA, accuracy: ± 0.01 m s⁻¹). Air temperature and soil

170 temperature at 0–1.0 m depth were also recorded by an automatic
171 microclimate gauging tower (CS3000, Campbell, USA) set in the center
172 part of the peatlands. Water level in the peatland was recorded
173 continuously near the gauging tower with the same Odyssey monitor. The
174 thaw depth of the peatland active layer was manually surveyed weekly
175 with a 1.0-m stainless steel ruler (accuracy: 0.1 cm) at the same three sites.
176 Information of the temperature ($^{\circ}\text{C}$), electrical conductivity (mS cm^{-1}), and
177 turbidity (NTU) in the sampling profile was logged continuously using a
178 multi-parameter water quality sonde (6600EDS, YSI, USA). About one-
179 fifth of the water quality data mainly in May and late September were lost
180 because of equipment malfunction at low temperature. All the instruments
181 were set to collect data every six hours while they were being deployed
182 while they were being deployed.

183

184 **2.3. Fluorescence measurements**

185 Excitation-emission matrixes (EEMs) of the water samples were
186 measured using a Hitachi F-7000 fluorescence spectrometer (Hitachi High
187 Technologies, Japan) with a 50 W ozone-free Xenon arc lamp and R928P
188 photomultiplier tube fitted as a detector. The spectrometer was set to collect
189 signals using a 5-nm bandpass on excitation and emission monochromators
190 at a scanning speed of $3,200 \text{ nm min}^{-1}$. EEMs were recorded for excitation

191 spectra of between 220 and 400 nm and for emission spectra of between
192 300 and 500 nm. To eliminate the inner-filter effect, samples were diluted
193 with deionized water to a UV absorbance at $\lambda = 254$ nm of 0.2 absorbance
194 units (cm^{-1}). Milli-Q water blank EEMs were subtracted from the sample
195 EEMs to eliminate Raman scatter peaks. Then, the EEMs were
196 normalized to the area under the Raman scatter peak (excitation
197 wavelength of 350 nm) of a Milli-Q water sample run the same day. The
198 fluorescence intensities measured were reported in Raman Units (RU) in
199 this study.

200 Three spectral indices were calculated from the EEMs to quantify
201 chemical characteristics of the dissolved organic matter. The humification
202 index (HIX) is defined as the ratio of the sum of $\lambda_{\text{em}} = 435\text{--}480$ nm to the
203 sum of $\lambda_{\text{em}} = 300\text{--}345$ nm for excitation at 254 nm and quantifies the
204 complexity and aromaticity of dissolved organic matter. High HIX values
205 denote the presence of highly humified or more complex organic matter
206 (Ohno, 2002). The fluorescence (FI) was the second index and is defined
207 as the ratio of fluorescence emission intensities at 470 and 520 nm for
208 excitation at 370 nm. The recommended FI for plant-derived organic
209 matter is 1.3-1.4 and that for materials of microbial origin is 1.7-2.0
210 (McKnight et al., 2001). The third index we measured was the biological
211 index (BIX), defined as the ratio of intensities at $\lambda_{\text{em}} 380$ nm and 430 nm
212 for excitation at 310 nm. BIX ranges from 0.6 to 1.0 or greater generally,

213 and is a complementary index for evaluating the relative contributions of
214 microbial-derived organic matter (Huguet et al., 2009). Lower values mean
215 proportionately less microbial-derived organic matter.

216 **2.4 Estimation of DOC load and yield**

217 A web-based program LOADEST was used to estimate the DOC load
218 for the three years (<https://engineering.purdue.edu/mapserve/LOADEST/>).
219 LOADEST uses linear regression models to identify relationships between
220 discharge and DOC concentrations, and in turn to estimate daily DOC load
221 by applying the statistical method of Adjusted Maximum Likelihood
222 Estimation (AMLE), Maximum Likelihood Estimation (MLE), and least
223 absolute deviation (LAD). In total, eleven models are used in the program,
224 and the best one was automatically selected to fit the data on the base of
225 Akaike Information Criterion (Park et al., 2015). In our study, 36, 35, and
226 31 measurements were used to calculate DOC loads for the years 2012,
227 2013, and 2014 respectively. Loads were estimated using the MLE method
228 according to the standard error (SE) and the distribution of the residuals.
229 The DOC yield was calculated as the load divided by the entire catchment
230 area.

231 **2.5. Statistical analyses**

232 The mean and the standard deviation of the DOC concentrations in the
233 stream and soil pore water, and the three fluorescence indices were

234 statistically analyzed with the Statistical Program for Social Sciences
235 (SPSS) version 13.0 software. The relationship between the hydrological
236 factors and the DOC concentration and the fluorescence indices was
237 examined by a two-tailed Pearson correlation and regression analysis,
238 where the p-values were calculated to test for significance. Analysis of
239 covariance (ANCOVA) was also conducted to distinguish if the
240 relationships between discharge and the DOC characteristics
241 (concentration and fluorescence indices) were statistically different for
242 different years, and if there were other factors controlling the DOC
243 characteristics besides discharge.

244

245 **3. Results**

246 **3.1. Environmental conditions**

247 Substantial inter-annual and seasonal variations in precipitation were
248 observed for the three years (Fig. 2). The total precipitation reached 202.5,
249 520.8 and 164 mm in 2012, 2013 and 2014, respectively. Based on our
250 statistics on the regional climate dataset from 1970 to 2005, 2013 was an
251 extremely wet year due to excessive rainfall occurring in the spring and
252 summer. The total rainfall in 2012 was within a normal range while that
253 for 2014 indicated an extreme dry year. Probably owing to the abundant
254 rainfall in 2013, the air temperature during the growing season in this year

255 with a mean value of 12.9°C, was lower than those of 2012 and 2014 (on
256 average 13.7°C). However, mean values in all three years were within the
257 average long-term range. We also found no significant differences in the
258 maximum thaw depths of soil active layer for the three years. The standing
259 water levels in the peatland close to the stream channel declined gradually
260 across the growing seasons probably due to the deepening of active layer.
261 Water levels in the peatland were always lower than peat surface during
262 the three years of sampling.

263

264 **Fig. 2 Air temperature, precipitation, water levels in peatland, and thaw**
265 **depth observed during the growing seasons of 2012 to 2014.**

266

267 **3.2. DOC concentrations and loads**

268 DOC concentrations in the Fukuqi River fluctuated considerably with
269 stream discharge during the three growing seasons (Fig. 3). The mean DOC
270 concentration in 2013 was significantly larger than that in 2012 and 2014
271 (Table 1). Great seasonal variability was clearly observed for all of the
272 three years, which mainly resulted from the varied rainfall patterns as
273 shown in Fig. 2. In the three years of measurements, the maximum
274 concentration of 44.7 mg L⁻¹ was found in the early spring of 2013 and was
275 accompanied by the peak flood occurring during the three years. The

276 estimated DOC loads and yields for the three years varied greatly (Table
277 1). The total load, as well as the DOC yield in the wet year of 2013 was
278 about six times that of the extreme dry year of 2014. The annual load and
279 yield in 2012 differed greatly compared with 2014, but the estimated mean
280 concentrations were quite similar. Monthly variability in loads was also
281 found, with maximum values occurring either in May or August. The mean
282 DOC load for the three years was $4.7 \text{ g m}^{-2} \text{ yr}^{-1}$. Several large floods
283 contributed the majority of the load. Statistically, nine flood events
284 (maximum discharge $> 1.0 \times 10^6 \text{ m}^3 \text{ d}^{-1}$) were responsible for 81% of the
285 load while five floods with a discharge level $> 2.0 \times 10^6 \text{ m}^3 \text{ d}^{-1}$ accounted
286 for 65% of the total load.

287

288 **Fig. 3** Dissolved organic carbon (DOC) concentrations and discharge (Q)
289 observed during the growing seasons of 2012 to 2014.

290

291 **Table 1.** Mean annual DOC loads, concentrations and yields estimated by
292 LOADEST program for 2012-2014.

293

294 Significant positive correlations were found between DOC
295 concentrations and discharge for all three growing seasons (Fig. 4).
296 However, results of covariance analysis suggested that the adjusted mean

297 DOC concentrations after eliminating the influence of discharge were
298 statistically different for the three years. This result suggested an inter-
299 annual variability in the linear relationship between DOC concentration
300 and discharge (Table 2). As indicated by Adj. R^2 , about sixty percentage of
301 the DOC variability could be explained by the discharge, and the
302 percentage was very similar for the three years. However, the mean
303 residuals for the three linear models were quite different. Tables 2 and 3
304 suggest that the greater mean residuals were accompanied by a wider
305 concentration range. Large concentration fluctuations would lead to a
306 decreased average predictive ability by discharge. DOC concentrations
307 were positively related to turbidity and negatively related to conductivity
308 ($n=68$, $p < 0.01$) while no significant relationship was found between the
309 concentrations and air temperature or the soil temperatures of active layer.

310

311 **Fig. 4 Relationships between discharge (Q) and the DOC concentrations**
312 **for 2012-2014 sampling periods.**

313

314 **Table 2. Results of covariance analysis (ANCOVA) between discharge and**
315 **the DOC concentrations for the 2012-2014 sampling periods.**

316

317 **Table 3. Results of linear regression analysis between discharge and the**

318 DOC concentrations for the 2012-2014 sampling periods.

319

320 **3.3. Fluorescence indices**

321 The three spectral indices varied considerably with discharge during
322 the growing seasons (Fig. 5). There was a significant positive correlation
323 between the HIX and logarithmic discharge but both FI and BIX were
324 negatively correlated with discharge for (Fig. 6). HIX ranged from 5.52 to
325 16.41 with an average value of 10.38, revealing a high proportion of more
326 humified components in the stream discharge DOC. FI and BIX values
327 ranged from 1.43 to 1.62 and from 0.46 to 0.63 with average values of 1.52
328 and 0.54, respectively. The FI values indicate that DOC originated both
329 from plant-derived organic matter and from microbial-mediated organic
330 matter while the BIX value denotes the presence of a low proportion of
331 young organic matter from biological sources in the discharge (see Huguet
332 et al., 2009). All three indices were closely related to DOC concentrations
333 and hydrological variables during the entire study period. Only HIX also
334 showed a significant relationship with soil temperature (Table 4). In spite
335 of the great variations during the three growing seasons, the mean annual
336 values of the three indices did not differ statistically for the three years
337 according to the covariance analysis, which eliminated the influence of
338 discharge (Table 5).

339

340 **Fig. 5** Dynamics of the three spectral indices following discharge (Q)
341 during the 2012- 2014 sampling period.

342

343 **Fig. 6** Relationships between discharge (Q) and the three indices during
344 the 2012-2014 study period.

345

346 **Table 4.** Correlation analysis of the three fluorescence indices with
347 hydrological and climatic factors.

348

349 **Table 5.** Results of covariance analysis (ANCOVA) between discharge and
350 the fluorescence indices for the study period.

351

352 **3.4. Concentrations and fluorescence indices of soil water**

353 During the growing seasons 2013, soil porewater DOC concentrations
354 in the three points presented similar vertical profiles. Maximum DOC
355 concentrations were typically found at the depth of 20-30 cm in the organic
356 soil layer while the minimum values were found at the deeper mineral layer
357 (Fig. 7). The vertical variation in DOC concentrations could be clearly
358 observed when the active layer reached the maximum depth in the early

359 autumn. However, no significant relationship was detected between DOC
360 concentration and soil temperature at different depths. The DOC
361 concentrations in the upper organic soil layer increased considerably from
362 early to late June, but did not change significantly from July to late August.
363 Across the entire growing seasons, no significant relationship was found
364 between the mean DOC concentration and the mean soil temperature in the
365 whole profile ($p > 0.05$, $n=4$).

366 The HIX, FI, and BIX of soil pore water varied greatly with soil depth
367 (Fig. 8). Pronounced changes in the three indices generally occurred at the
368 depth where organic soil transitioned to the mineral soil. HIX values
369 gradually decreased with depth while FI and BIX increased with depth.
370 The fluorescence indices in the upper organic soil layer changed
371 significantly during the growing seasons. However, no consistent from
372 spring to autumn was found. The mean values for the three indices were
373 16.62, 1.41, and 0.46 respectively in 2013. The data indicated a much
374 higher HIX level and a lower FI and BIX level in soil pore water than in
375 the baseflow stream discharge. HIX values were significantly and
376 positively correlated to DOC concentrations in soil pore water while FI and
377 BIX were significantly but inversely and correlated with DOC
378 concentrations ($n = 18$, $p < 0.01$).

379

380 **Fig. 7 DOC concentrations in soil pore water along the vertical soil profile**
381 **in 2013.**

382

383 **Fig. 8 Distribution of the three spectral indices for vertical soil pore water**
384 **profiles in 2013.**

385

386 **4. Discussion**

387 **4.1. DOC concentrations and yield**

388 DOC concentrations in boreal rivers have been reported to vary
389 considerably according to differences in hydrology, soil type and
390 topography (Andersson and Nyberg, 2008; Tunaley et al., 2016; Broder et
391 al., 2017). Theoretically, the presence of organic soils in the catchment
392 should contribute to higher DOC concentrations in connected rivers.
393 However, no direct relationship between organic soil content and mean
394 DOC concentration was extensively found across the boreal regions. In
395 our study, the annual mean concentration, 15.4 mg L⁻¹, was in the middle
396 of the range of concentrations reported from boreal regions, from 1.5 to
397 35.3 mg L⁻¹ (Yates et al., 2016; Avagyan et al., 2016). The DOC yield
398 from our catchment was estimated at 4.7 g m⁻² yr⁻¹, which was in the lower
399 range of estimates reported for permafrost region, which ranged from 1 to
400 35 g m⁻¹ yr⁻¹ (Fraser et al., 2001; Dinsmore et al., 2010; Moody et al.,

401 2016). The mean DOC yield in our catchment was less than the net DOC
402 loss reported from UK lands ($2.1-11.5 \text{ g m}^{-2} \text{ yr}^{-1}$) (Moody et al., 2013), but
403 it was higher than in Finnish rivers ($3.5 \text{ g m}^{-2} \text{ yr}^{-1}$) (Räike et al., 2012), in
404 the Yukon River in Alaska ($1.4-3.7 \text{ g m}^{-2} \text{ yr}^{-1}$) (Striegl et al., 2007), and in
405 central Siberian rivers ($2.8-4.7 \text{ g m}^{-2} \text{ yr}^{-1}$) (Prokushkin et al., 2011). Pan
406 Arctic rivers exported 32 Tg C yr^{-1} of DOC to the Arctic Ocean according
407 to estimates by Kichlighter et al. (2013), which indicated a mean yield of
408 $5.1 \text{ g m}^{-2} \text{ yr}^{-1}$ from the north Eurasian permafrost. Our results indicated
409 there was a slightly lower DOC yield in the southern part of the Eurasian
410 permafrost. However, our data are representative only of the region in
411 northeastern China. More field studies are needed to better estimate DOC
412 loads from the entire south Eurasia permafrost region.

413 Miao (2014) estimated the net ecosystem exchange (NEE) between
414 peatland surfaces and the atmosphere using both carbon dioxide and
415 methane fluxes was $30.59 \pm 1.98 \text{ g m}^{-2} \text{ yr}^{-1}$ in the study catchment.
416 Therefore, the estimated DOC yield in our study accounted roughly for
417 18.3% of the net ecosystem carbon balance in the entire catchment. As the
418 upland mountains, extensively covered by mineral soils, likely export
419 little DOC to the stream compared with the peatland, the actual DOC yield
420 based on the extent of the peatland will be much higher than $4.7 \text{ g m}^{-2} \text{ yr}^{-1}$.
421 Therefore, the yield generated by our study is a very conservative
422 estimate. Even so, our data still demonstrated the significant contribution

423 of stream carbon export to the net peatland ecosystem carbon balance.
424 Any disturbance altering DOC export processes and magnitudes will
425 disrupt the balance between carbon sequestration and release in the
426 Eurasia peatlands. The proportion of stream carbon export in our study
427 was much higher than that in a northwest Russia river for which the DOC
428 exported by streamflow accounted for 5.6-8.5% of the total carbon
429 sequestration in the peatlands (Avagyan et al., 2016), but it was close to a
430 peat catchment in Scotland, in which DOC represented a loss of 24% of
431 NEE (Dinsmore et al., 2010).

432

433 **4.2. Flow pathways, DOC sources and chemical characteristics**

434 Peatlands in permafrost regions generally experience subsurface flows
435 but not overland flows due to high rainfall infiltration into the thawed
436 organic layer (Carey and Woo, 1997). In our study, the porosity of peat in
437 the upper 40 cm layer was between 20-60%, which would necessarily
438 allow rapid and high infiltration of rainfall. The infiltrating rainfall was
439 blocked from further vertical flow by the frozen soil, and as a result flowed
440 laterally towards the stream. Lateral subsurface flow was an essential
441 prerequisite for the positive relationship between discharge and the DOC
442 concentrations to avoid the dilution effect which would result from
443 overland flow (Guo et al., 2015).

444 The three fluorescence indices, HIX, FI, and BIX, exhibited
445 considerable fluctuations during rainfall-runoff events in our study,
446 implying shifts in DOC sources and chemical characteristics during
447 subsurface flow. The three indices varied vertically within the organic soil
448 layer up to the mineral layer. Vertical trends were maintained throughout
449 the growing season of 2013 (Fig. 8). This pattern made the indices good
450 indicators of DOC sources. Given the significant correlation between the
451 indices and discharge, we concluded that the DOC released during flood
452 periods originated mostly from the upper organic soil layer, whereas the
453 DOC during recession and baseflow periods originated mainly from the
454 lower mineral layer. Carey and Woo (2001) described permafrost soil as a
455 two-layer flow system based on the difference in hydraulic conductivity
456 between the upper organic soil and lower mineral soil: Quickflow, defined
457 as matrix flow or preferential flow in interconnecting soil pipes and rills,
458 took place in the highly porous peat in the upper layer, while slowflow was
459 laminar flow in the lower saturated mineral soils where flow velocities
460 were orders of magnitude lower than quickflow. As the porosity declined
461 exponentially in the transition from organic to mineral soil in the studied
462 peatland, soil pore water in the upper organic soil with high concentrations
463 of DOC should be transported by quickflow during floods, while baseflow
464 conditions had much lower DOC concentrations from the deeper mineral
465 soil.

466 Seasonal shifts in DOC sources and composition have been reported
467 in previous studies in permafrost catchments (Spencer et al., 2008;
468 O'Donnell et al., 2010). However, our results highlighted the importance
469 of the shifts temporally during runoff event. In our study, the deepening of
470 the soil active layer with thaw led to the presence of vertical discontinuity
471 in hydraulic conductivity in the discharge-yield profile, and to shifts in
472 DOC sources and chemical characteristics during runoff. Because there
473 were only a few rainfall events in 2014, we were able to identify the effects
474 of the gradual deepening of the active layer during the growing season as
475 the thawing proceeded. Significant increases in BIX and FI values during
476 baseflow occurred from the spring to the autumn in 2014 (Fig. 4). This
477 implied a concomitant increase in the proportion of microbial-derived
478 DOC as the active layer deepened. During thawing of the active layer, the
479 hydraulic residence time and the DOC mineralization rate, as well as
480 physical adsorption in the mineral soil would increase (Cronan and Aiken,
481 1985; Sebestyen et al., 2008), and this would alter DOC chemical
482 characteristics under baseflow conditions. The fact that DOC in soil pore
483 water exhibited higher HIX values and lower FI and BIX values compared
484 to that in the baseflow discharge was direct proof of adsorption-
485 mineralization in the mineral soil layer. DOC humification decreased and
486 microbial-derived components increased when DOC was delivered by
487 slowflow across the mineral soil. Our result is consistent with the study of

488 Prokushkin et al. (2007) who also found higher levels of microbially
489 transformed and/or derived material export due to the presence of a deeper
490 active layer in the summer and autumn in Siberia. Changes in biochemical
491 composition (decreases in the lignocellulose complex; increases in the
492 hydrophilic fraction) were also confirmed by Kawahigashi et al. (2004).
493 Based on these observations, a 9-11% reduction in DOC load due to
494 permafrost degradation was predicted in the Yukon River by 2050
495 (Walvoord and Striegl, 2007), and an increase in dissolved inorganic
496 carbon was also hypothesized (Striegl et al., 2005). From these
497 observations we infer that deepening of the active layer in a warming
498 climate conceivably could reduce DOC export by baseflow, as well as alter
499 DOC chemical characteristics to more structure-simple microbial-derived
500 components in the study region.

501 The HIX index for DOC showed no clear seasonal trend in the
502 anomalously dry year of 2014. Even a minor flood caused a large increase
503 in HIX, implying the sensitivity of DOC chemical characteristics to the
504 shift in the primary flowpath from quickflow to slowflow. The previous
505 analysis had highlighted the importance of the seasonal thawing of the
506 active layer to flowpaths and DOC chemical characteristics. Covariance
507 analysis showed that the discharge quantity was the sole factor leading to
508 inter-annual variations in the DOC chemical characteristics. There was no
509 significant difference in the maximum thaw depths of the active layer for

510 any of the three years (Fig. 2), which was likely the reason why inter-
511 annual effect of active layer thawing could not be distinguished. In total,
512 we conclude that there were different controlling factors on DOC chemical
513 characteristics depending on different temporal scales. Long-term field
514 investigations are crucially needed to evaluate in-depth the influence of
515 permafrost thaw on prevailing flowpaths and chemical characteristics of
516 DOC.

517

518 **4.3. Discharge and DOC export**

519 We found a significant positive relationship between DOC
520 concentration and stream discharge, which is consistent with results
521 observed in other permafrost regions (Hinton et al., 1998; Petrone et al.,
522 2007; Balcarczyk et al., 2009; Koch et al., 2013). The positive relationship
523 occurred in both the wet and the dry year, suggesting that DOC export from
524 the studied catchment is a transport-limited process. Specifically, DOC
525 transport capacity was mainly related to processes that controlled runoff,
526 for example flow path, rate of runoff and lag time. As described earlier, the
527 flowpath-shift was an equally important mechanism contributing to the
528 positive relationship between discharge and DOC concentrations. Our
529 conclusion is supported by both DOC model simulations (Neff and Asner,
530 2001; Wu, et al., 2014) and field experiments (Tipping et al., 1999),

531 reporting linear increases in DOC concentrations with increasing amounts
532 of subsurface flow.

533 It may be hypothesized that DOC is being generated in the peatland in
534 amounts large enough to make up for the loss of the DOC exported by
535 successive floods in the growing seasons. It is noteworthy that DOC
536 concentrations were consistently high in stream discharge during
537 successive big floods in the autumn of 2012 and the spring of 2013.
538 Meanwhile, the DOC concentrations in the organic soil layer of the
539 peatland remained at a stable high level about 40 mg L⁻¹ through the
540 growing seasons. Successive rainfalls and seasonal temperature variations
541 did not result in decreased concentrations in the peatland (Fig. 7). These
542 data demonstrate the large DOC productive potential of the peat soil.

543 The regression slopes for the positive relationships between DOC and
544 discharge showed large inter-annual variations (Fig. 4). The results of
545 covariance analysis indicated that were other factors besides discharge
546 quantity underlay inter-annual variations. The high sensitivity of DOC
547 production and degradation to temperature was well established (see
548 Kalbitz et al., 2000; Moore et al., 2008). However, in our study no
549 significant relationships were found between the mean temperature and the
550 mean residual concentrations in the regression formulations for all three
551 years (Table 3). Therefore temperature could not explain the residual
552 variations. Precipitation also was shown to be of great importance for DOC

553 dynamics in boreal peatlands (for example Olefeldt et al., 2013; Pumpanen
554 et al., 2014). Discharge during flood events can mobilize large quantities
555 of pre-event water stored in the riparian zone (Kirchner, 2003; Winterdahl
556 et al., 2011), and both the time interval of two successive rainfalls and the
557 quantity of the antecedent rainfall could influence DOC concentrations in
558 the second flood. It is possible that rainfall frequency during the growing
559 seasons could exert a cumulative effect on annual DOC dynamics.
560 However, our data did not provide conclusive evidence and more detailed
561 and longer study is needed in this regard. Nevertheless, the positive
562 relationship between annual discharge and annual mean DOC
563 concentrations ($p < 0.05$, $n=3$) (Fig. 9) provided a simple tool to estimate
564 annual DOC load in the catchment.

565

566 **Fig. 9 Relationship between annual discharge (Q) and DOC load for the**
567 **three years.**

568

569 **5. Conclusions**

570 Eurasian permafrost serves as an important potential carbon pool for
571 the atmosphere and for linked aquatic and ocean ecosystems.
572 Investigations of DOC responses in permafrost peatland could be used to
573 predict the ecological consequences of climatic change in these regions.

|

574 Our study investigated the loads and determinants of DOC export from a
575 peatland catchment along the southern margins of Eurasian permafrost.
576 The catchment exhibited a relatively low DOC load compared to other
577 permafrost regions, and the yield estimates were an important contribution
578 for estimating global fluvial carbon export. DOC export in our study
579 catchment was transport-limited process as indicated by the positive
580 correlation between discharge and DOC concentrations in both wet and dry
581 years. Field investigations indicated that the source of the DOC and its
582 chemical characteristics were greatly influenced by the flowpath shifts
583 between the upper organic soil layer and the lower mineral layer. The shifts
584 were closely related to the vertical soil structure and seasonal thawing of
585 the active layer. Deepening of active layer following permafrost
586 degradation would increase the content of microbial-originated DOC in
587 baseflow discharge by increasing the relative contribution from the lower
588 mineral soil layer to the DOC pool. Our study has provided limited field
589 data on DOC dynamics in the southern region of Eurasian permafrost.
590 Additional more intensive studies are needed to improve our understanding
591 and predictions of the dynamics of DOC under future climate change.

592

593 **Acknowledgements**

594 The work was supported by National Key Research and Development

595 Program of China (2016YFA0602303), National Natural Science
596 Foundation of China (41571097, 41730643), Key of Frontier Sciences,
597 Chinese Academy of Sciences (QYZDJ-SSW-DQC013), Research
598 Program of Northeast Institute of Geography and Agroecology, Chinese
599 Academy of Science (IGA-135-05).

600

601

602 **References**

603 Ågren, A., Haei, M., Köhler, S. J., Bishop, K., Laudon, H.: Regulation of
604 stream water dissolved organic carbon (DOC) concentrations during
605 snowmelt; the role of discharge, winter climate and memory effects,
606 *Biogeosciences*, 7, 2901–2913, 2010.

607 Avagyan, A., Runkle, B. R. K., Hennings, N., Haupt, H., Virtanen, T.,
608 Kutzbach, L.: Dissolved organic matter dynamics during the spring
609 snowmelt at a boreal river valley mire complex in Northwest Russia,
610 *Hydrol. Process.*, 30, 1727–1741, 2016.

611 Andersson, J-O., Nyberg, L.: Spatial variation of wetlands and flux of
612 dissolved organic carbon in boreal headwater streams, *Hydrol. Process.*,
613 22,1965–1975, 2008. DOI:10.1002/hyp.6779.

614 Balcarczyk, K.L., Jones Jr, J.B., Jaffé, R., Maie, N.: Stream dissolved
615 organic matter bioavailability and composition in watersheds underlain

616 with discontinuous permafrost, *Biogeochemistry*, 94, 255–270, 2009.

617 Broder, T., Knorr, K. H., Biester, H.: Changes in dissolved organic matter
618 quality in a peatland and forested headwater stream as a seasonality and
619 hydrologic conditions, *Hydrol. Earth Syst. Sci.*, 21, 2035–2051, 2017.

620 Carey, S., Woo, M.K.: Snowmelt hydrology of two subarctic slopes,
621 Southern Yukon, Canada. In *Proceedings of the Eleventh Northern
622 Research Basins Symposium and Workshop (Vol 2)*, Prudhoe
623 Bay/Fairbanks Alaska. The Water and Environmental Research Centre,
624 University of Alaska, Fairbanks, pp. 15–35, 1997.

625 Carey, S.K., Woo, M.K.: Slope runoff processes and flow generation in a
626 subarctic, subalpine catchment, *J. Hydrol.*, 253, 110–129, 2001.

627 Cory, R.M., Ward, C.P., Crump, B.C., Kling, G.W.: Sunlight controls
628 water column processing of carbon in arctic fresh waters, *Science*, 345,
629 925–928, 2014.

630 Cronan, C.S., Aiken, G.R.: Chemistry and transport of soluble humic
631 substances in forested watersheds of the Adirondack Park, New York,
632 *Geochim. Cosmochim. Acta*, 49, 1697–1705, 1985.

633 Dinsmore, K.J., Billett, M.F., Skiba, U.M., Rees, R.M., Drewer, J., Helfter,
634 C.: Role of the aquatic pathway in the carbon and greenhouse gas
635 budgets of a peatland catchment, *Global Change Biol.*, 16, 2750–2762,
636 2010.

- 637 Frey, K. E., McClelland, J. W.: Impacts of permafrost degradation on arctic
638 river biogeochemistry, *Hydrol. Process.*, 23, 169–182, 2009.
- 639 Fraser, C.J.D., Roulet, N.T., Moore, T.R.: Hydrology and dissolved
640 organic carbon biogeochemistry in an ombrotrophic bog, *Hydrol.*
641 *Process.*, 15, 3151–3166, 2001.
- 642 Guo, Y.D., Song, C.C., Wan, Z.M., Tan, W.W., Lu, Y.Z., Qiao, T.H.:
643 Effects of long-term land use change on dissolved carbon
644 characteristics in the permafrost streams of northeast China, *Environ.*
645 *Sci.: Processes Impacts*, 16, 2496–2506, 16, 2014.
- 646 Guo, Y.D., Song, C.C., Wan, Z.M., Lu, Y.Z., Qiao, T.H., Tan, W.W.,
647 Wang, L.L.: Dynamics of dissolved organic carbon release from a
648 permafrost wetland catchment in northeast China. *J. Hydrol.*, 531, 919–
649 928, 2015.
- 650 Hinton, M.J., Schiff, S.L., English, M.C.: Sources and flowpaths of
651 dissolved organic carbon during storms in two forested watersheds of
652 the Precambrian Shield. *Biogeochemistry*, 41, 175–197, 1998.
653 doi:10.1023/A:1005903428956
- 654 Huguet, A., Vacher, L., Relexans, S., Saubusse, S., Froidefond, J.M.,
655 Parlanti, E.: Properties of fluorescent dissolved organic matter in the
656 Gironde Estuary, *Org. Geochem.*, 40, 706–719, 2009.
- 657 Jin, H.J., Li, S.X., Cheng, G.D., Wang, S.L., Li, X.: Permafrost and

658 climatic change in China, *Global Planet., Change* 26, 387–404, 2000.

659 Kalbitz, K., Soliiger, S., Park, J.H., Michalzik, B., Matzner, E.: Controls
660 on the dynamics of dissolved organic matter in soils: A review, *Soil Sci.*,
661 165, 277–304, 2000.

662 Kalbitz, K., Schwesig, D., Rethemeyer, J., Matzner, E.: Stabilization of
663 dissolved organic matter by sorption to the mineral soil, *Soil Biol*
664 *Biochem.*, 37, 1319–1331, 2005.

665 Kawahigashi, M., Kaiser, K., Kalbitz, K., Rodionov, A., Guggenberger, G.:
666 Dissolved organic matter in small streams along a gradient from
667 discontinuous to continuous permafrost, *Global Change Biol.*, 10,
668 1576–1586, 2004.

669 Kicklighter, D. W., Hayes, D. J., McClelland, J. W., Peterson, B. J.,
670 McGuire, A. D., Melillo, J. M.: Insights and issues with simulating
671 terrestrial DOC loading of Arctic river networks, *Ecol. Appl.*, 23,
672 1817–1836, 2013.

673 Kirchner, J.W.: A double paradox in catchment hydrology and
674 geochemistry, *Hydrol. Processes*, 17, 871–874, 2003.

675 Koch, J.C., Runkel, R.L., Striegl, R., McKnight, D.M.: Hydrologic
676 controls on the transport and cycling of carbon and nitrogen in a boreal
677 catchment underlain by continuous permafrost, *J. Geophys. Res-Biogeo.*,
678 118, 698–712, 2013. doi:10.1002/jgrg.20058,

- 679 Laudon, H., Berggren, M., Ågren, A., Buffam, I., Bishop, K., Grabs, T.,
680 Jansson, M., Köhler, S.: Patterns and dynamics of dissolved organic
681 carbon (DOC) in boreal streams: the role of processes, connectivity,
682 and scaling, *Ecosystems*, 14, 880–893, 2011.
- 683 Lessels, J.S., Tetzlaff, D., Carey, S.K., Smith, P., Soulsby, C.: A coupled
684 hydrology-biogeochemistry model to simulate dissolved carbon
685 exports from a permafrost-influenced catchment. *Hydro. Process.*, 29,
686 5383–5396, 2015.
- 687 Lyon, S. W., Destouni, G., Giesler, R., Humborg, C., Mörth, M., Seibert,
688 J., Karlsson, J., and Troch, P. A.: Estimation of permafrost thawing
689 rates in a sub-arctic catchment using recession flow analysis, *Hydrol.*
690 *Earth Syst. Sci.*, 13, 595–604, 2009.
- 691 Lyon, S.W., Morth, M., Humborg, C., Giesler, R., Destouni, G.: The
692 relationship between subsurface hydrology and dissolved carbon fluxes
693 for a sub-arctic catchment, *Hydrol. Earth Syst. SC.*, 14, 941–950, 2010.
- 694 Mann, P.J., Davydova, A., Zimov, N., Spence, R.G.M., Davydov, S.,
695 Bulygina, E., Zimov, S., Holmes, R.M.: Controls on the composition
696 and liability of dissolved organic matter in Siberia’s Kolyma river basin,
697 *J. Geophys. Res-Bioge.*, 117, G01028, 2012. doi:
698 10.1029/2011JG001798.
- 699 McKnight, D. M., Boyer, E. W., Westerhoff, P. K., Doran, P. T., Kulbe, T.,

700 and Andersen, D. T.: Spectrofluorometric characterization of dissolved
701 organic matter for indication of precursor organic material and
702 aromaticity, *Limnol. Oceanogr.*, 46, 38–48, 2001.
703 doi:10.4319/lo.2001.46.1.0038.

704 Miao, Y.Q.: Net ecosystem carbon fluxes of peatland in the continuous
705 permafrost zone, Great Hinggan Mountains. Dissertation. University of
706 Chinese Academy of Sciences. pp, 120, 2014. (in Chinese)

707 Moody, C.S., Worrall, F., Burt, T.P.: Identifying DOC gains and losses
708 during a 20-year record in the Trout Beck catchment, Moor House, UK,
709 *Ecol. Indic.*, 68, 102–114, 2016.

710 Moody, C.S., Worrall, F., Evas, C.D., Jones, T.G.: The rate of loss of
711 dissolved organic carbon (DOC) through a catchment, *J. Hydrol.*, 492,
712 139–150, 2013.

713 Moore, T. R., Paré, D., and Boutin R.: Production of dissolved organic
714 carbon in Canadian forest soils, *Ecosystems*, 11, 740–751, 2008.

715 Neff, J. C. and Asner, G. P.: Dissolved organic carbon in terrestrial
716 ecosystems: synthesis and a model, *Ecosystems*, 4, 29–48, 2001.

717 Ohno, T.: Fluorescence inner-filtering correction for determining the
718 humification index of dissolved organic matter, *Environ. Sci. Technol.*,
719 36, 742–746, 2002.

720 O'Donnell, J. A., Aiken, G. R., Kane, E. S., Jones, J. B.: Source water

721 controls on the character and origin of dissolved organic matter in
722 streams of the Yukon River basin, Alaska, *J. Geophys. Res.*, 115,
723 G03025, 2010. doi:10.1029/2009JG001153.

724 Olefeldt, D., Roulet, N., Giesler, R., Persson, A.: Total waterborne c
725 arbon export and DOC composition from ten nested subarctic peatland
726 catchments-importance of peatland cover, groundwater influence, and
727 inter-annual variability of precipitation patterns. *Hydrol. Process.*, 27,
728 2280–2294, 2013.

729 Opsahl, S., Benner R., Amon R. M. W.: Major flux of terrigenous dissolved
730 organic matter through the Arctic Ocean, *Limnol. Oceanogr.*, 44,
731 2017–2023, 1999.

732 Park, Y.S., Engel, B.A., Frankenberger, J., Hwang, H.: A-web-based tool
733 to estimate pollutant loading using LOADEST, *Water*, 7, 4858-4868,
734 2015. doi:10.3390/w7094858.

735 Petrone, K.C., Jones, J.B., Hinzman, L.D., Boone, R.D.: Seasonal export
736 of carbon, nitrogen, and major solutes from Alaskan catchments with
737 discontinuous permafrost, *J. Geophys. Res.*, 111, G02020, 2006.
738 doi:10.1029/2005JG000055.

739 Petrone, K.C., Hinzman, L.D., Shibata, H., Jones, J.B., Boone, R.: The
740 influence of fire and permafrost on sub-arctic stream chemistry during
741 storms, *Hydrol. Process.*, 21, 423–434, 2007. doi:10.1002/hyp.6247.

742 Prokushkin, A.S., Pokrovsky, O. S., Shirokova, L.S., Korets, M.A., Viers,
743 J., Prokushkin, S.G., Amon, R. M. W., Guggenberger, G., McDowell,
744 W.H.: Sources and the flux pattern of dissolved carbon in rivers of the
745 Yenisey basin draining the Central Siberian Plateau, *Environ. Res.*
746 *Lett.*, 6, 045212, 2011. doi:10.1088/1748-9326/6/4/045212.

747 Prokushkin, A.S., Gleixner, G., McDowell, W.H., Ruehlow, S., Schulze,
748 E.D.: Source and substrate-specific export of dissolved organic matter
749 from permafrost-dominated forested watershed in central Siberia,
750 *Global Biogeochem. Cy.*, 103, 109–124, 2007.

751 Pumpanen, J., Linden, A., Miettinen, H., Kolari, P., Ilvesniemi, H.,
752 Mammarella, I., Hari, P., Nikinmaa, E., Heinonsalo, J., Back, J., Ojala,
753 A., Berninger, F., Vesala, T.: Precipitation and net ecosystem exchange
754 are the most important drivers of DOC flux in upland boreal
755 catchments, *J. Geophys. Res-Bioge.* 119, 1861-1878, 2014.

756 Räike, A., Kortelainen, P., Mattsson, T., David N. Thomas, D. N.: 36 year
757 trends in dissolved organic carbon export from Finnish rivers to the
758 Baltic Sea, *Sci. Total Environ.*, 435–436, 188–201, 2012.

759 Sebestyen, S.D., Boyer, E.W., Shanley, J.B., Kendall, C., Doctor, D.H.,
760 Aiken, G.R., Ohte, N.: Sources, transformations and hydrological
761 processes that control stream nitrate and dissolved organic matter
762 concentrations during snowmelt in an upland forest, *Water Resour. Res.*,

763 44, W12410, 2008. doi:10.1029/2008WR006983.

764 Spencer, R. G. M., Aiken, G. R., Wickland, K. P., Striegl, R. G., Hernes,
765 P. J.: Seasonal and spatial variability in dissolved organic matter
766 quantity and composition from the Yukon River basin, Alaska, *Global*
767 *Biogeochem. Cycles*, 22, GB4002, doi:10.1029/2008GB003231, 2008.

768 Spencer, R.G., Mann, P.J., Dittmar, T., Eglinton, T.I., McIntyre, C.,
769 Holmes, R.M., Zimov, N., Stubbins, A.: Detecting the signature of
770 permafrost thaw in Arctic rivers, *Geophys. Res. Lett.*, 42(8), 2830–
771 2835, 2015.

772 Striegl, R. G., Aiken, G. R., Dornblaser, M. M., Raymond, P. A., Wickland,
773 K. P.: A decrease in discharge-normalized DOC export by the Yukon
774 River during summer through autumn, *Geophys. Res. Lett.*, 32, L21413,
775 2005. doi:10.1029/2005GL024413.

776 Striegl, R. G., Dornblaser, M. M., Aiken, G. R., Wickland, K. P., Raymond,
777 P. A.: Carbon export and cycling by the Yukon, Tanana, and Porcupine
778 rivers, Alaska 2001–2005, *Water Resour. Res.*, 43, W02411, 2007.
779 doi:10.1029/2006WR00.

780 Tipping, E., Woof, C., Rigg, E., Harrison, A. F., Inneson, P., Taylor, K.,
781 Benham, D., Poskitt, J., Rowland, A. P., Bol, R., and Harkness, D. D.:
782 Climatic influences on the leaching of dissolved organic matter from
783 upland UK moorland soils, investigated by a field manipulation

784 experiment, *Environ. Inter.*, 25, 83–95, 1999.

785 Townsend-Small, A., McClelland, J. W., Max Holmes, R., Peterson, B. J.:
786 Seasonal and hydrologic drivers of dissolved organic matter and
787 nutrients in the upper Kuparuk River, Alaskan Arctic, *Biogeochemistry*,
788 103, 109–124, 2011.

789 Tunaley, C., Tetzlaff, D., Lessels, J., Soulsby, C.: Linking highfrequency
790 DOC dynamics to the age of connected water sources, *Water Resour.*
791 *Res.*, 52, 5232–5247, 2016.

792 Vonk, J.E., Mann, P.J., Davydov, S., Davydova, A., Spencer, R.G.M.,
793 Schade, J., Sobczak, W.V., Zimov, N., Zimov, S., Bulygina, E.,
794 Eglinton, T.I.: High biolability of ancient permafrost carbon upon thaw,
795 *Geophys. Res. Lett.*, 40, 2689–2693, 2013.

796 Walvoord, M. A., Striegl, R. G.: Increased groundwater to stream
797 discharge from permafrost thawing in the Yukon River basin: Potential
798 impacts on lateral export of carbon and nitrogen, *Geophys. Res. Lett.*,
799 34, L12402, 2007. doi:10.1029/2007GL030216.

800 Winterdahl, M., Futter, M., Köhler, S., Laudon, H., Seibert, J., Kevin
801 Bishop, K.: Riparian soil temperature modification of the relationship
802 between flow and dissolved organic carbon concentration in a boreal
803 stream. *Water Resour. Res.*, 47, W08532, 2011.
804 doi:10.1029/2010WR010235.

805 Wu, H., Peng, C., Moore, T.R., Hua, D., Li, C., Zhu, Q., Peichl, M., Arain,
806 M.A., Guo, Z.: Modeling dissolved organic carbon in temperate forest
807 soils: TRIPLEX-DOC model development and validation, *Geosci.*
808 *Model Dev.*, 7, 867–881, 2014.

809 Yates, C.A., Johnes, P.J., Spencer, R. G. M.: Assessing the drivers of
810 dissolved organic matter export from two contrasting lowland
811 catchments, U.K, *Sci. Total Environ.*, 569–570, 1330–1340, 2016.

812

813

814

815

816

817 **Table 1.** Mean annual DOC loads, concentrations and yields estimated by LOADEST

818 program for 2012-2014.

Period	Load (Kg)			Concentration (mg L ⁻¹)			Yield (g m ⁻²)		
	SE			CV (%)			SE		
	2012	2013	2014	2012	2013	2014	2012	2013	2014
May	1388	66502	4238	9.00	35.49	15.04	0.08	6.02	0.40
	<i>161</i>	<i>7479</i>	<i>194</i>	<i>39.3</i>	<i>25.2</i>	<i>30.5</i>	<i>0.009</i>	<i>0.13</i>	<i>0.06</i>
June	5917	3728	3574	16.53	17.92	15.88	0.62	0.39	0.37
	<i>619</i>	<i>235</i>	<i>164</i>	<i>30.4</i>	<i>26.0</i>	<i>16.4</i>	<i>0.02</i>	<i>0.07</i>	<i>0.07</i>
July	3372	12228	4056	14.08	16.76	15.02	0.36	1.32	0.44
	<i>268</i>	<i>1261</i>	<i>191</i>	<i>26.9</i>	<i>19.6</i>	<i>24.0</i>	<i>0.09</i>	<i>0.04</i>	<i>0.07</i>
August	9385	14475	2194	13.35	16.14	11.32	1.01	1.56	0.24
	<i>982</i>	<i>1394</i>	<i>95</i>	<i>48.1</i>	<i>49.8</i>	<i>12.7</i>	<i>0.03</i>	<i>0.15</i>	<i>0.03</i>
September	8788	3875	1977	11.12	13.49	10.09	0.77	0.38	0.19
	<i>870</i>	<i>471</i>	<i>106</i>	<i>48.3</i>	<i>26.7</i>	<i>11.3</i>	<i>0.03</i>	<i>0.03</i>	<i>0.03</i>
Annual	6092	19022	3211	13.26	19.57	13.48	2.84	9.68	1.64
	<i>423</i>	<i>1521</i>	<i>89</i>	<i>38.6</i>	<i>29.4</i>	<i>19.0</i>	<i>0.18</i>	<i>0.38</i>	<i>0.26</i>

819

820

821

822

823

824

825

826

827

828

829

830

831

832 **Table 2** Results of covariance analysis (ANCOVA) between discharge and the DOC
833 concentrations for the 2012-2014 sampling periods.

Source	Sum of squares	df	Mean squares	F.	Sig.
Corrected model	2895.334	3	965.111	41.213	0.000
Log ₁₀ Q	2026.994	1	2026.994	86.559	0.000
Year	303.294	2	151.647	6.476	0.002
Error	2294.932	98	23.418		

834 DOC concentrations and log₁₀Q are dependent variable and covariate respectively; Year
835 denotes fixed factor; Adjusted mean annual concentrations for the three years are
836 15.25±0.88, 18.32±0.84, and 14.22±0.81 mg L⁻¹ in turn.

837

838

839 **Table 3.** Results of linear regression analysis between discharge and the DOC
840 concentrations for the 2012-2014 sampling periods.

Model	2012			2013			2014		
	DF	Sum of Squares	Mean Square	DF	Sum of Squares	Mean Square	DF	Sum of Squares	Mean Square
Regression	1	690.85	690.85	1	1582.96	1582.96	1	271.18	271.18
Residual	34	558.21	16.45	33	1032.80	31.30	29	185.92	6.41
Total	35	1249.06		34	2615.76		30	457.10	

841

842

843

844

845

846

847 **Table 4.** Correlation analysis of the three fluorescence indices with hydrological and
 848 climatic factors.

		DOC	Q	Conductivity	Turbidity	T _{air}	T _{soil}
HIX	Pearson	0.708**	0.609*	0.451**	-0.592**	0.342	0.395*
	Sig. (2-tailed)	0.000	0.000	0.005	0.000	0.115	0.02
	n	92	92	68	68	92	92
FI	Pearson	-0.594**	-0.606**	-0.477**	0.469**	0.353	0.389
	Sig. (2-tailed)	0.000	0.000	0.004	0.001	0.203	0.128
	n	92	92	68	68	92	92
BIX	Pearson	-0.64**	-0.707**	-0.488**	0.322*	-0.027	0.384
	Sig. (2-tailed)	0.001	0.000	0.001	0.012	0.823	0.129
	n	92	92	68	68	92	92

849 DOC is dissolved organic carbon; Q is stream discharge; T_{air} is the average air
 850 temperature over the past three days; T_{soil} is the average soil temperature of the active
 851 layer; “***” denotes p < 0.01; “*” denotes p < 0.05

852

853

854

855

856 **Table 5.** Results of covariance analysis (ANCOVA) between discharge and the
857 fluorescence indices for the study period.

Index	Source	Sum of squares	df	F.	Sig.
HIX	Log ₁₀ Q	296.045	1	70.315	0.000
	Year	9.318	2	1.107	0.335
FI	Log ₁₀ Q	0.097	1	63.490	0.000
	Year	0.007	2	2.128	0.125
BIX	Log ₁₀ Q	0.084	1	86.098	0.000
	Year	0.004	2	1.850	0.163

858

859 The indices, HIX, FI, and BIX, are set as dependent variables; log₁₀Q is covariate; Year
860 denotes fixed factor.

861

862

863

864

865

866

867

868

869
870
871
872
873
874
875
876
877
878
879
880
881
882
883
884
885
886
887
888
889
890
891
892
893
894
895
896
897
898
899
900
901
902
903
904
905
906
907
908

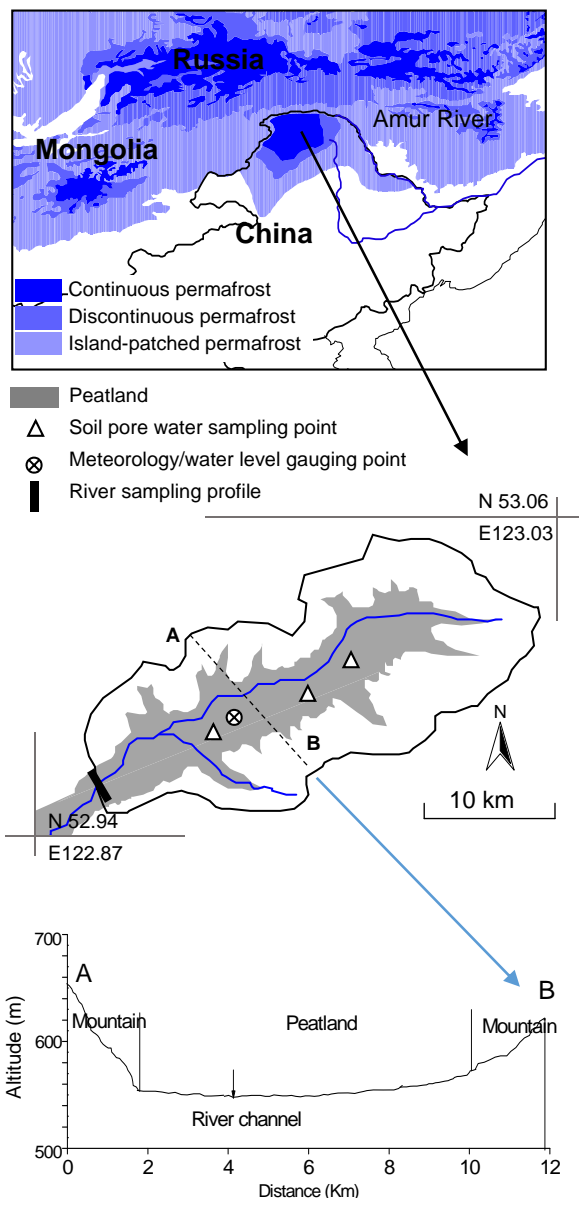


Fig. 1 Geographic location of the study area

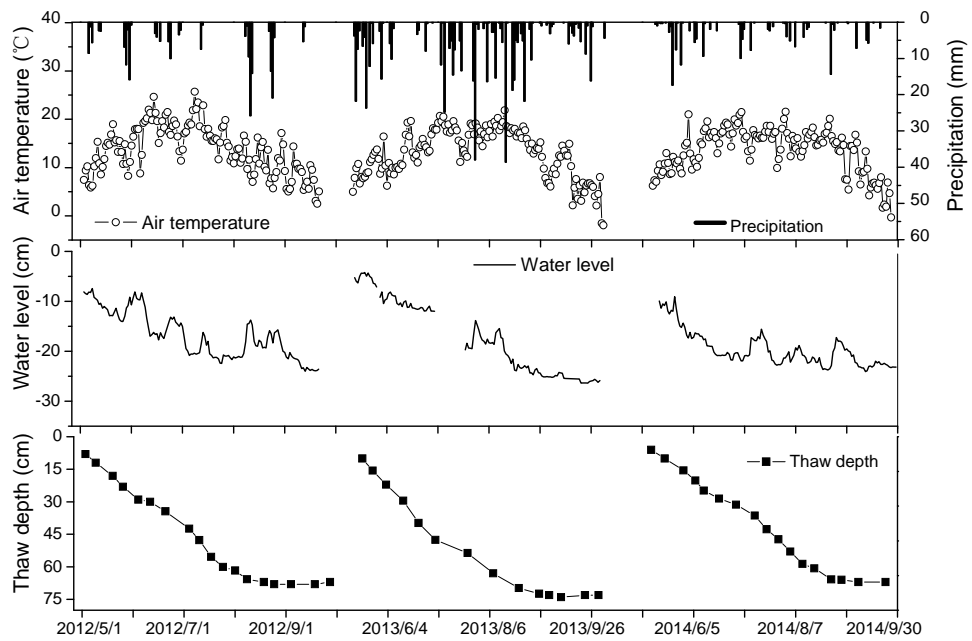


Fig. 2 Air temperature, precipitation, water levels in peatland, and thaw depth observed during the growing seasons of 2012 to 2014.

927

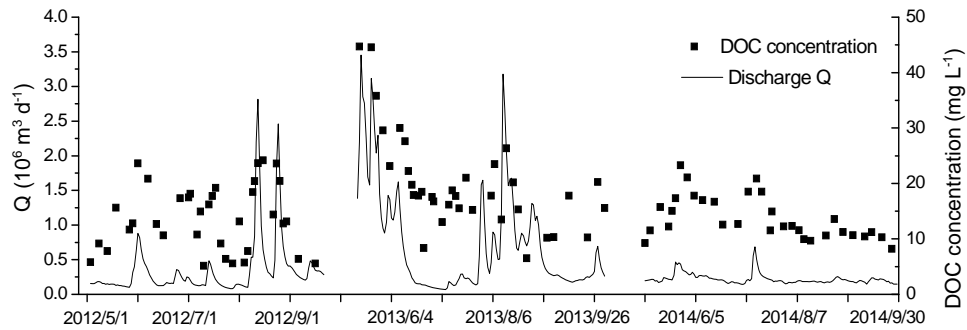
928

929

930

931

932



933 **Fig. 3** Dissolved organic carbon (DOC) concentrations and discharge (Q) observed
934 during the growing seasons of 2012 to 2014.

935

936

937

938

939

940

941

942

943

944

945

946

947

948

949

950
951
952
954
955
956
957
958
959
960
961
962
963
964
965
966
967
968
969
970
971
972
973
974
975
976

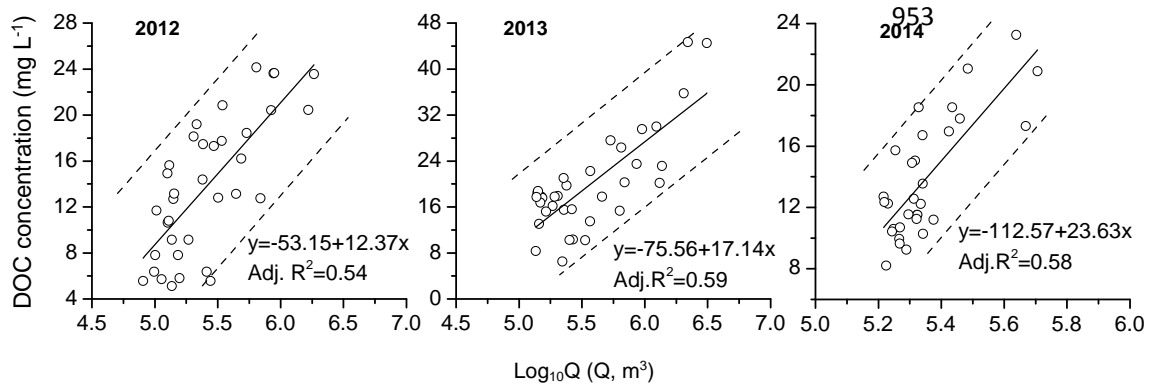


Fig. 4 Relationships between discharge (Q) and the DOC concentrations for 2012-2014 sampling periods.

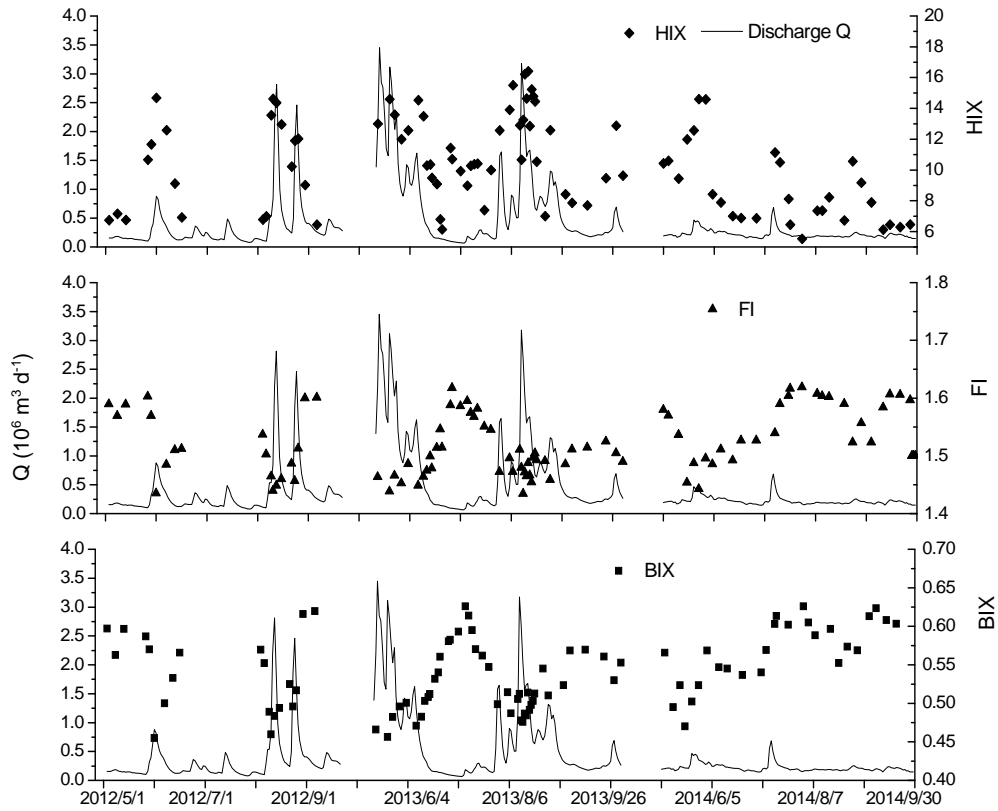
977

978

979

980

981



982

983

984

985

986

987

988 **Fig. 5** Dynamics of the three spectral indices following discharge (Q) during the 2012-

989 2014 sampling period.

990

991

992

993

994

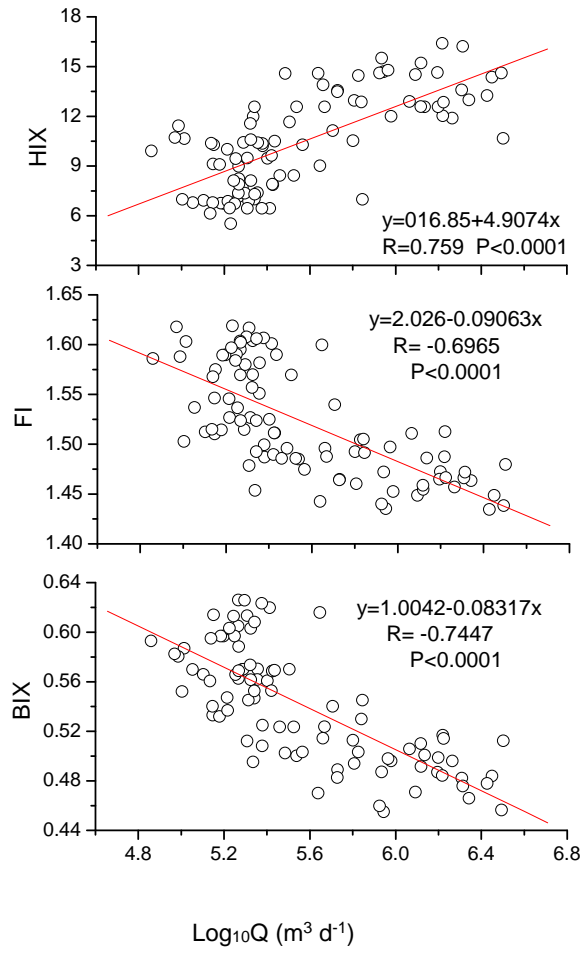
995

996

997

998

999



1000

1001

1002

1003

1004

1005

1006

1007 **Fig. 6** Relationships between discharge (Q) and the three indices during the 2012-2014

1008 sampling period.

1009

1010

1011

1012

|

1013

1014

1015

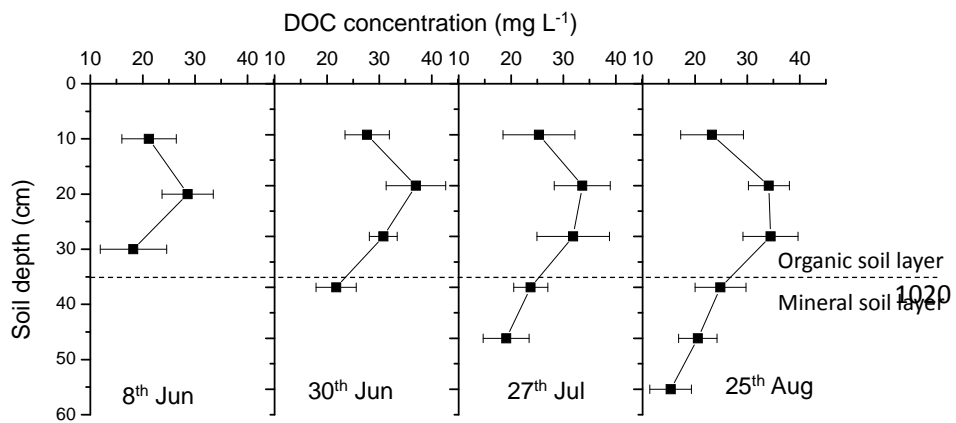
1016

1017

1018

1019

1021



1022

1023 **Fig. 7** DOC concentrations in soil pore water along the soil profile in 2013.

1024

1025

1026

1027

1028

1029

1030

|

1031

1032

1033

1034

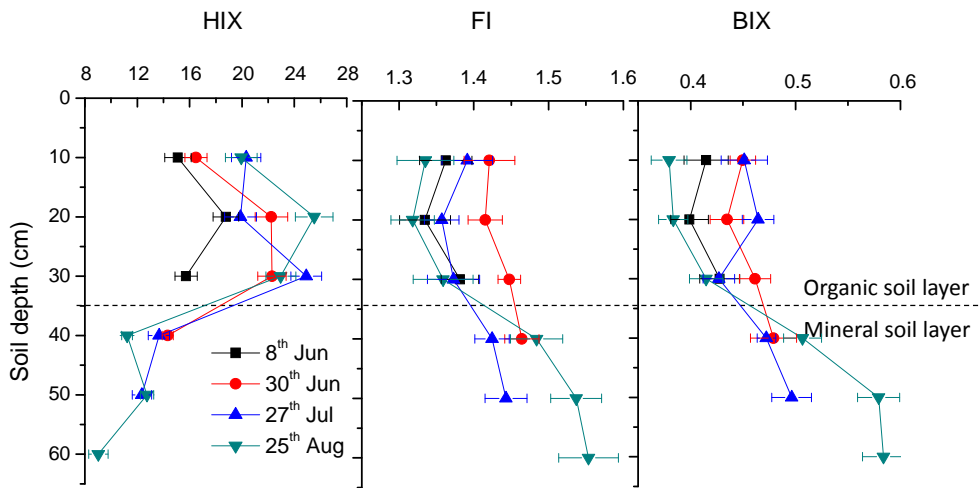
1035

1036

1037

1038

1039



1040 **Fig. 8** Vertical distribution of the three spectral indices for soil pore water along the soil
1041 profile in 2013.

1042

1043

1044

1045

1046

1047

1048

1049

|

1050

1051

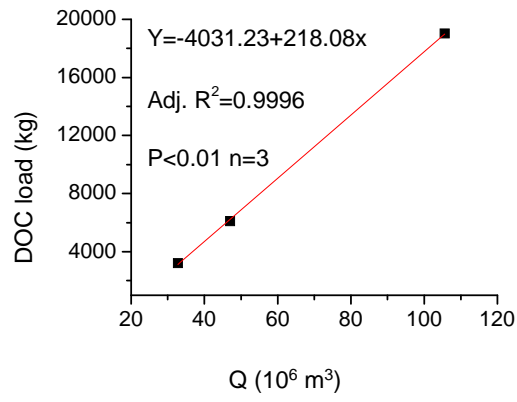
1052

1053

1054

1055

1056



1057 **Fig. 9** Relationship between annual discharge (Q) and DOC load for the three years.

1058

1059